

ORGANIC MATTER VARIATIONS IN A TRANSGRESSIVE SYSTEM TRACK: AN EXAMPLE OF THE ALMOND FORMATION, ROCK SPRINGS UPLIFT, WYOMING (U.S.A.)

García, G. M.¹

ABSTRACT

The oil-prone coals of the Almond Formation are studied using sequence stratigraphy and organic geochemistry. The occurrence of the organic facies (defined with geochemical and maceral analyses) is related to four-order parasequences of the Almond Formation. Hydrogen index and macerals content trends are useful tools in identifying four-order unconformities.

Key words: Almond formation, organic facies, hydrogen Index, liptinite, desmocollinite, vitrinite reflectance suppression.

VARIACIONES DE LA MATERIA ORGÁNICA EN UNA SECUENCIA DE UN SISTEMA TRANSGRESIVO: UN EJEMPLO DE LA FORMACIÓN ALMOND, ROCK SPRINGS UPLIFT, WYOMING (U.S.A.)

RESUMEN

Los mantos de carbón de la formación Almond en Rock Springs Wyoming fueron estudiados empleando técnicas de estratigrafía de secuencias y geoquímica orgánica. Los resultados ilustran una relación entre la facies orgánica (definidas mediante análisis geoquímicos y análisis de macerales) y la presencia de inconformidades de cuarto orden de la Formación Almond. En este sentido se observó como las tendencias del índice de hidrógeno y el contenido y composición maceral son buenos parámetros para identificar límites de parasecuencias de la Formación Almond.

Palabras claves: Facies orgánicas, índice de hidrogeno, liptinita, desmocollinita, supresión de la reflectancia de vitrinita

¹ Escuela de Geología, Universidad Industrial de Santander A. A. 678, Bucaramanga, Colombia.
Correo electrónico: mgarciag@uis.edu.co

INTRODUCTION

This paper focuses on the variability organic matter in the overall transgressive Almond Formation of the Mesaverde Group in the Washakie Basin. Also it is studied the relationship between organic facies and the distribution of oil-and-gas source rocks in a succession. Special attention is paid to coal beds that are oil-prone according to García-González et al. (1997 and 1993).

Olson and Martinsen (1999) and Olson (1999) analyzed the stratigraphy of the Almond Formation and attempted to subdivide the succession into four-order sequences by means of identifying several intervals on the basis of stratigraphic concepts. This paper presents the organic facies determined from geochemical analyses and organic petrography of the Almond Formation coal, and uses these criteria to identify four-order sequences in the Almond Formation.

Geochemical and organic petrographical analyses were carried out with samples taken from the UW # 4 cored well, which was drilled near the south end of the Rock Springs Uplift in Wyoming (FIGURE 1).

The oil-prone coals of the Almond Formation are revisited and characterized using sequence stratigraphy and organic geochemistry. The organic facies variability is used to test the sequentiality suggested by Olson (1999).

GEOLOGICAL SETTING

The Greater Green River Basin (GGRB) lies in the Rocky Mountain Foreland. Its present structural configuration is the result of tectonics of the Overthrust Belt during the Laramide Orogeny during late Cretaceous and early Tertiary time. The Foreland was broken into a number of smaller basins by basement-involved thrusting and folding. Highlands were elevated and exposed to erosion, and sediments were transported into the newly formed intermountain basins (Roehler, 1990).

The GGRB includes four intrabasin uplifts (the north-trending Moxa Arch and Rock Springs Uplift and the east-trending Wamsutter Arch and Cherokee Arch) and four sub-basins (the Green River, Cherokee, Washakie, and Sand Wash Basins) (FIGURE 1).

The Rock Springs uplift is a north-south trending foreland structure of 65 miles (104 km) long and 30 miles (48 km) wide. Major structural features near the Rock Springs Uplift include: on the east side, the Great Divide Basin, Wamsutter Arch, Washakie Basin, and Sand Wash Basin, these last three structures are being bounded eastward by the Rawlins, Sierra Madre, and North Park uplifts. The major structures west of the Rock Springs Uplift are: Pinedale anticline, Green River basin, Moxa Arch, and the Wyoming-Idaho Overthrust belt (FIGURE 1).

In age the strata of the GGRB range from Cambrian to Tertiary. Some were buried to a depth of 32,000 ft (9,750 m). Most of these sedimentary rocks are of Upper Cretaceous, Paleocene, or Eocene age (Tyler et al., 1992).

In the GGRB, coal-bearing intervals are collectively thousands of feet thick, and they extend from the Upper Cretaceous Mesaverde Group through the Lower Tertiary Wasatch Formation. The thickest and most continuous Cretaceous coal beds occur in the Mesaverde Group, which includes the Williams Fork, Almond, Rock Springs, and Lance formations (FIGURE 2).

The Mesaverde Group consists of stacked wedges of siliclastic sediments interfingering with pelitic sediment that prograded from the area of the Siever orogenic belt (Utah) eastward into the Cretaceous Western Interior Seaway, as illustrated in Figure 3. Crabaugh (1988) interpreted these siliclastic wedges as third order sequences.

Most of the sediments composing the Mesaverde Group were deposited along the western margins of the interior Cretaceous seaway, where extensive marine transgressions, and regressions, took place over a period of 13 million years during Campanian and Maastrichtian times.

STRATIGRAPHY OF THE ALMOND FORMATION

The Almond Formation is Upper Campanian to lower Maastrichtian in age ranging from 70 to 72.5 M.a. according to Obradovich (1993). This age was determined on the basis of ammonite zones established by Gill, et al. (1970), in Roehler, (1990).

TABLE 1. Maceral analyses of Almond Formation Coals.

Sample No	Depth ft	Desm. %	Collin. %	Tellin. %	Liptin. %	resinite %	exsud %	Fusini %	semifus %	micri %	macri %	Vitrinite %	Liptinite %	Inertinite %	Clays %	Pyrite %	Miners %	Total %	
	0	0.0																	
UW#4 97	-97	59.0	12.4		5.7	4.8		9.5	6.7	1.9		71.4	10.5	18.1				0.0	100.0
UW#4 99	-99	32.1	44.9	1.3	10.3	2.6				9.0		78.3	12.9	9.0				0.0	100.2
UW#4 100	-100	39.8	29.0		8.7	4.3		5.4	7.5	2.2	1.1	68.8	13.0	16.2		2.2		2.2	100.2
UW#4 101	-101	42.6	35.7	6.1	8.6	1.7	0.8	1.7	0.8	1.7		84.4	11.1	4.2				0.0	99.7
UW#4 125	-125	33.8	39.6	8.6	10.1	1.4	0.7	1.4		3.6		82.0	12.2	5.0	0.7			0.7	99.9
UW#4 129	-129	26.3	25.4	11.9	2.5			4.2	10.2	2.5		63.6	2.5	17.0	15.3	1.7		17.0	100.1
UW#4 259	-259	24.0	48.0		14.0					2.0		72.0	14.0	2.0	8.0	4.0		12.0	100.0
UW#4 316	-316	26.2	44.8	1.2	8.1	3.5		2.3	4.7	2.3	0.6	72.2	11.6	9.9	4.7	1.7		6.4	100.1
UW#4 316-317	-317	32.9	40.3		10.1	4.3		5.8	2.9	1.4	0.7	73.2	14.4	10.8	1.4	0.7		2.1	100.5
UW#4 323	-323	30.8	48.0		9.6			7.7	1.0		2.9	78.8	9.6	11.6				0.0	100.0
UW#4 375	-375	28.4	53.2		5.5			5.5	2.8	4.6		81.6	5.5	12.9				0.0	100.0
UW#4 390	-390	25.0	61.0	8.0	2.0			6.0	1.0	3.0		94.0	2.0	10.0				0.0	106.0
UW#4 392	-392	13.0	55.1		11.6			1.4	7.2	2.8	2.8	68.1	11.6	14.2				0.0	93.9
UW#4 412-416	-412	18.8	42.4		4.7			8.2	8.2	4.7	3.6	61.2	4.7	24.7	9.4			9.4	100.0
UW#4 413-16	-413	9.1	34.1	10.2	5.6			8.0	9.1	3.4	4.6	53.4	5.6	25.1	15.9			15.9	100.0
UW#4 412-16	-416	37.1		40.0	5.7		5.7	2.6	8.6			77.1	11.4	11.2				0.0	99.7
UW#4 424	-424	15.4	50.8	24.6					1.5	3.1		90.8	0.0	4.6	1.5			1.5	96.9
UW#4 458	-458	27.1			2.1			8.3	2.1	4.2		27.1	2.1	14.6	54.2	2.1		56.3	100.1
UW#4 465-467	-465	14.1	41.2	40.0	2.4				1.2			95.3	2.4	1.2				0.0	98.9
UW#4 465-467	-467	22.6	54.8		11.3			4.8		6.5		77.4	11.3	11.3				0.0	100.0
UW#4 499-503	-499	14.4	48.9		4.0			16.6	8.8	1.1	1.1	63.3	4.0	27.6	2.2	2.2		4.4	99.3
UW#4 549	-549	20.4	56.1	7.1	4.1			2.0	2.0	4.1	4.1	83.6	4.1	12.2				0.0	99.9
UW#4 580	-580	8.4	68.1	11.1	5.6			1.4				87.5	5.6	1.4	5.6			5.6	100.1

Organic matter variations in a transgressive system track: An example of the Almond Formation, Rock Springs Uplift, Wyoming (U.S.A.)

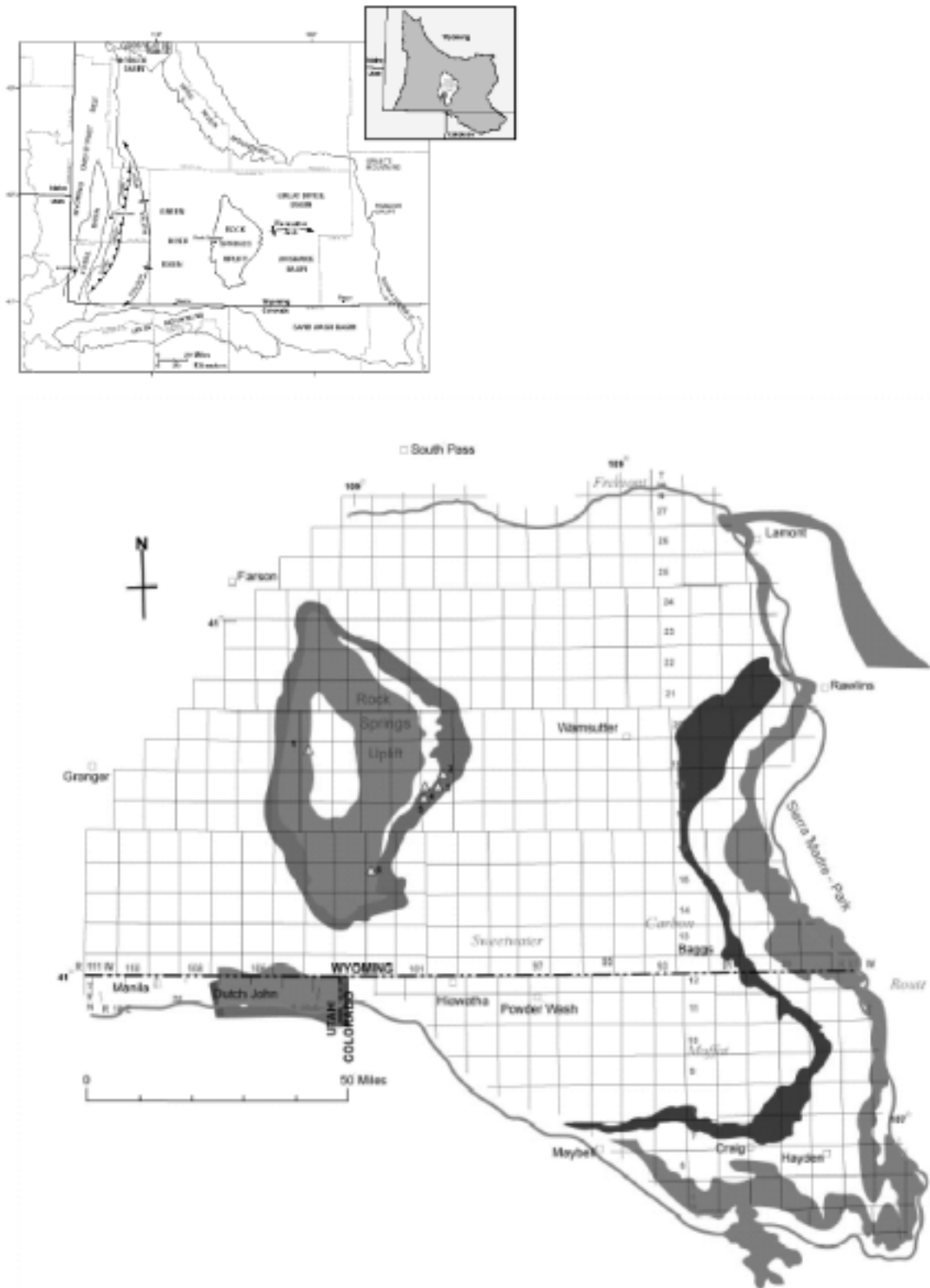


FIGURE 1. Location of outcrops and UW # 4 well

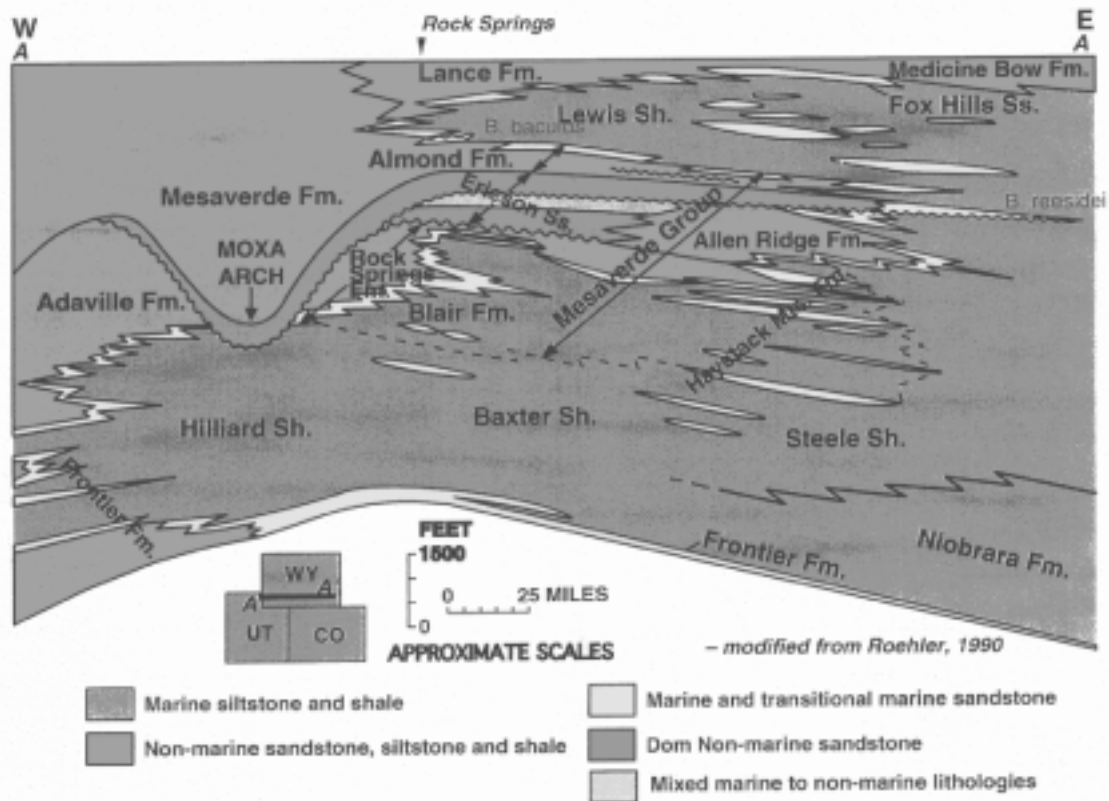


FIGURE 2. Cross section showing an interpretation of Roehler (1990) of the Upper Cretaceous Formations across northern Utah and South Wyoming

The marine Lewis Shale overlies the Almond Formation. Because of landward stepping of successive high-frequency sequences, the contact of these two formations young seaward (Roehler, 1990).

On the Rock Springs Uplift, the Almond Formation is underlying by the Canyon Creek Member of the Ericson Formation. The contact between the Ericson and the Almond Formations is sharp with minor or no topographic relief, and is placed between the top of the uppermost cross-stratified sandstone bed-set and the first thick succession of silty carbonaceous shales with thin coal beds, Olson (1999).

Flores, 1978, Van Horn, 1979 and Roehler, 1990 have previously divided the Almond Formation in the Rock Springs Uplift area into two mappable members: the Upper Member characterized by sandstones, and the Lower Member consisting predominantly of shales, coal, siltstones, and sandstones. The contact between these two members is unconformable, Van Horn (1979).

The inter-tonguing of Lewis Shales with the Upper Almond sands further subdivides the upper Almond into various sandstone units, each of which pinches out into the Lewis Shale east of the Rock Springs Uplift. Van Horn (1979) studied the Almond in the northern Rock Springs Uplift and western Washakie basin, and he named the Upper Almond sandstone successions as UA-1, UA-2, and UA-3 from youngest to oldest. Roehler (1988), named the upper sandstone succession (outcropping in the southeastern Rock Springs Uplift area) as barrier bars AA through G. Barrier bars G and F Roehler (1988) are tentatively correlated with UA-3 sandstone unit of Van Horn 1979. Therefore, on the basis of this correlation, the base of the Upper Almond is at located near the base of the Barrier bar G.

Sequence stratigraphy framework of the Almond Formation

The Almond Formation corresponds to the transgressive limb of a large-scale, third order clastic wedge of the Mesaverde Group, with a maximum span in age of 2 M.a. in the Rock Springs Uplift. The formation was

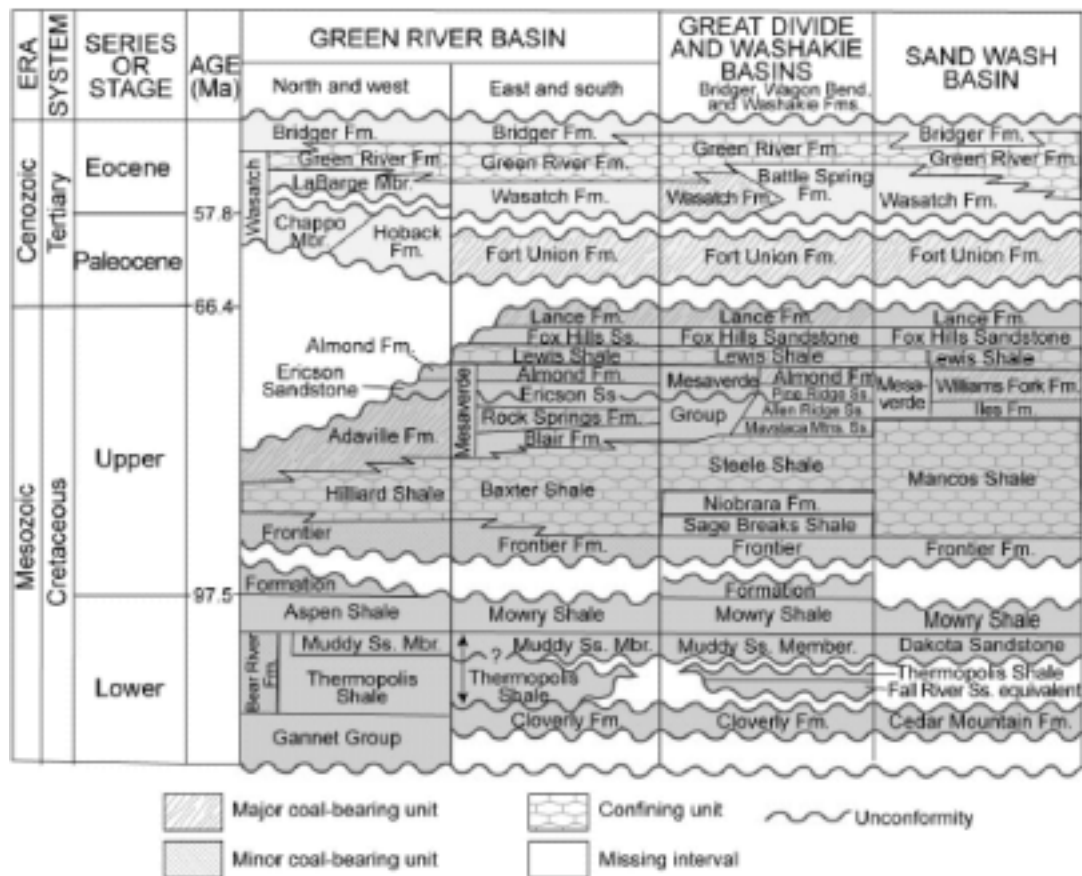


FIGURE 3. Coal-bearing stratigraphic units in the Greater Green River Basin (From Scott A, 1995).

deposited during an overall transgression, and is characterized by a series of individually regressive tongues or parasequences, as illustrated in FIGURE 4.

In the UW # 4 well, the Almond Formation can be subdivided into fourth-order sequences by flooding surfaces, creating three informal stratigraphic units: Lower, Middle and Upper Almond Formation as illustrated in FIGURE 5. This subdivision is the result of minor transgressive and regressive events identified within the overall transgressive systems tract of the Almond Formation.

The Lower Almond consists of multiple units of very fine sandstones that grade upward into siltstones. Cross stratification and ripple laminae are the common structures. The Lower Almond changes from fluvial channel sandstone at the base to carbonaceous shales in the middle and shaley siltstones at the top. This sequence was deposited mainly during transgression. The contact between the Lower and Middle Almond is marked by an unconformity.

The Middle Almond shows a predominance of back-barrier facies that start at the base with fluvial channel sandstones and over bank shales. This succession ends with the appearance of multiple thin coal beds. The overlying succession is shaley siltstone, carbonaceous shales, and sporadic thin coal beds that were formed in swamps, marshes and tidal flat depositional settings. This unit was also deposited in a transgressive system tract stage.

The Upper Almond starts with tidal sandstones at the base, followed by a succession of shaley sandstones and carbonaceous shales, deposited in a lagoonal environment. Overlying this succession, there is a succession of shore sediments that consist of upper and lower shoreface sandstones. The top of this unit shows an interfingering of lower shore face sandstone and offshore shales. This unit was deposited as a high stand system track stage (HST).

DEPOSITIONAL ENVIRONMENTS OF THE ALMOND FORMATION

The depositional environments of the Almond Formation on the southern Rock Springs Uplift start with a coastal plain environment that gradually changes upwards to back-barrier environment. Upwards the back-barrier environment changes to an open marine shoreline, and gradually to the offshore shales of the Lewis Formation.

The Lower Almond consists of several fining-upward packages of fine sandstone and siltstone, with cross stratification and ripple laminae, to shales and carbonaceous shales. Olson (1999) interpreted these deposits as coastal plain, and related fluvial, swamp and marsh environments.

The top of the Lower Almond is defined by a flooding surface, where the conditions change from fluvial water to brackish-water environments due to a rise in the sea level as indicated by the presence of tidal flat siltstone (Meyer, 1977; Flores, 1978; Van Horne, 1979).

The Middle Almond Formation contains three successions. The first was deposited in coastal plain and back-barrier environments. It consists of several fining-upward packages of sandstone, siltstone and shales with cross stratification and ripple lamination.

The second succession was deposited in marsh and swamp environments with some marine flooding; it consists of siltstone and shale interbedded with thin sandstone layers. The sandstone layers are moderate to intensely bioturbated. Also thin coal beds are interbedded in this succession.

The top of the Middle Almond includes a package of fine-grained sandstones with abundant clay rip-up clasts (intraclasts) characteristic of tidal channels.

The Upper Almond Formation consists initially of a succession of siltstones, shales and coal beds at the lower segment. The siltstones show ripple lamination and bioturbation. Shales are laminated and rich in organic matter. In the UW # 4 well, eight coal beds are present in this part of the Upper Almond.

The upper segment of the third parasequence is sand prone, but also with four coal beds. The predominant lithology is very fine sandstone that gradually coarsens upwards to medium-grained sandstone. The stratification alternates between cross stratification and hummocky stratification. Bioturbation is more abundant than in the Middle and Lower Almond. The upper sandstones are relatively thick and consist of two (at the UW # 4 well) or more stacked succession. This sandstone shows increasing abundance of bioturbation,

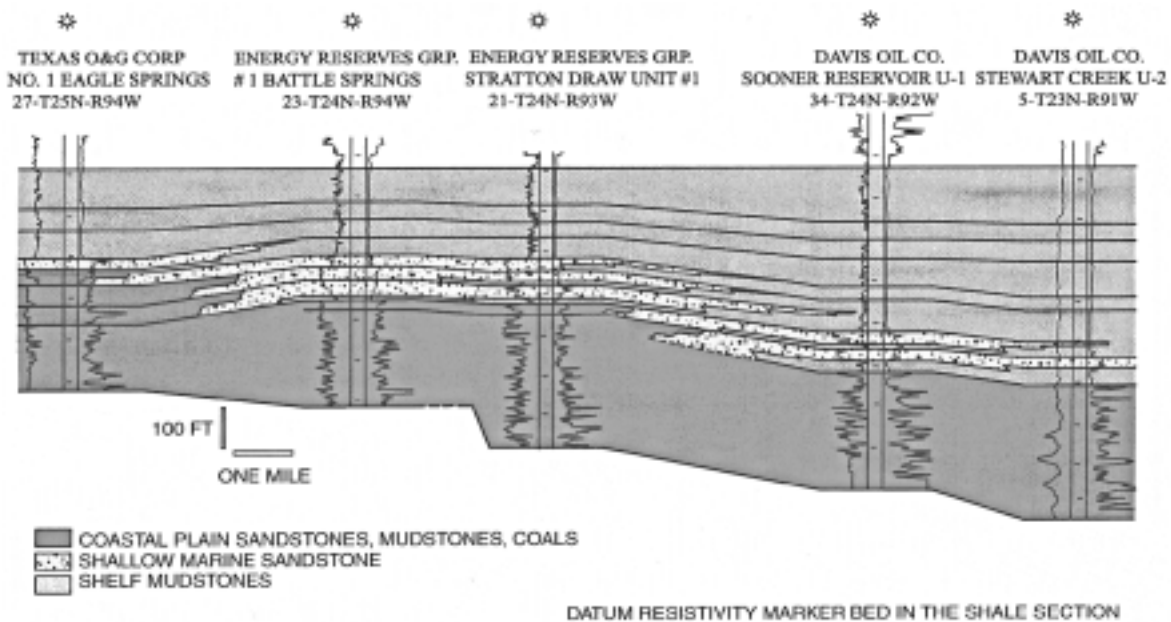


FIGURE 4. West to East log cross-section of the Almond Formation, Washakie Basin, illustrating the landward stepping parasequences. (From Martinsen et al., 1995)

including: Planolites, Ophiomorpha, Asterosoma, Teichichnus, and Zoophycos, and also dinoflagellates (Meyers, 1977).

The depositional environments identified by Olson (1999) in the Upper Almond starts at the base with marsh, and lagoon environments with some marine influence. This environment resulted in thin coal beds interstratified with carbonaceous shale and siltstone. The upper segment represents a shore face environment that is cut by siltstone and fine grain sandstone of a tidal inlet. The upper part of the Upper Almond contains only two coal beds that were deposited in a lagoonal environment.

The Upper Almond was deposited along a micro to low meso-tidal coastline characterized by chains of

barrier islands with closely spaced and actively migrating tidal inlets (Flores, 1978; Van Horn, 1979; Roehler, 1988; Weimer et al., 1965, 1988).

COAL PETROGRAPHY

The petrologic studies of the Almond coals and shales were performed with reflection microscopy under white and blue light on polished pellet composed of 4.75-mm-diameter (plus 10-mesh) coal particles. The petrographic analyses include identification of nine maceral, vitrinite reflectance measurements, along with textural description.

TABLE 1 summarizes the maceral point-count data from coal beds. The Lower Almond shows vitrinite content ranging from 63 to 88%. The liptinite content

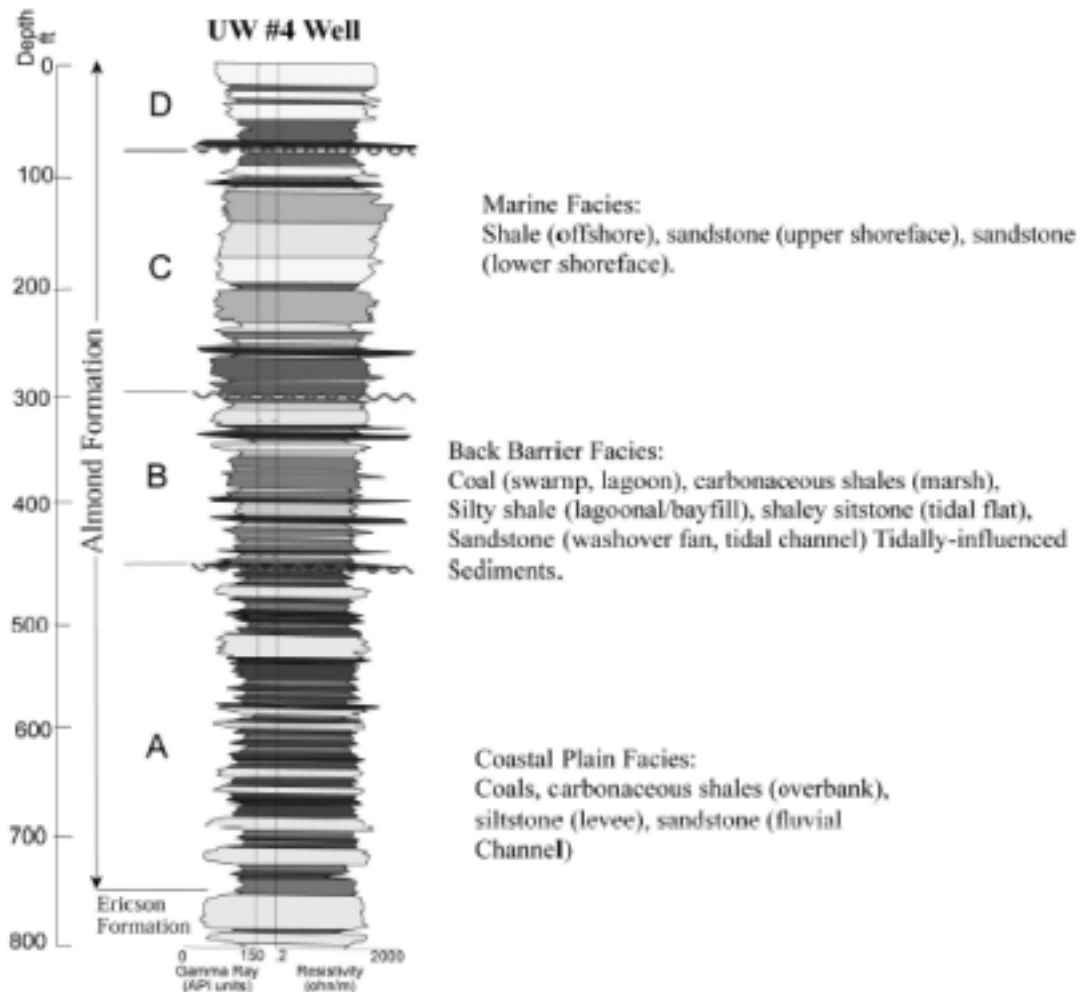


FIGURE 5. U.W core well # 4, gamma-ray/resistivity log and facies of Almond Formation.

is low (4 – 6%), and the inertinite content varies between 1.4 to 27%. The Middle coal beds present the following maceral composition: vitrinite 53 to 91%, liptinite 1 to 11%, and inertinite varies from 1 to 24%. The Upper Almond coal beds show a maceral composition that ranges in vitrinite content from 77 to 91% with liptinite ranging between 2 and 12.5 and inertinite between 4 and 11%.

The maceral content variation was plotted against depth, and two distinctive trends are observed for liptinite and desmocollinite (hydrogen-rich vitrinite) as illustrated in FIGURES 6 and 7. The liptinite content increases upward in the coal beds for both the Middle and Upper Almond units. This same trend is also clear for desmocollinite content, which increases from base to top on both Middle and Upper Almond, (FIGURES 6, and 7).

While the inertinite content does not present a clear trend, its maximum content exists in the Lower Almond coal beds. The inertinite content varies from 2 to 27 % and is composed mainly of fusinite and semifusinite.

The coaly shales thus present TOC values of between 10 and 50% and are an excellent source rock for hydrocarbons. Petrographically, these coaly shales are characterized by laminar texture in which vitrinite laminae are interbedded with shale or clay laminae, as illustrated by the photomicrograph in FIGURE 8. The coaly shale of the Almond Formation shows fluorescence of amorphous kerogen and also from oil-saturated clay minerals.

The Almond coals show commonly a laminar texture composed of alternating bright and dull bands. At the microscopic scale the laminar texture is also observed especially in the desmocollinite-rich coals, see photomicrograph of FIGURE 9, which increases from bottom to top of the Formation. Desmocollinite is the most abundant vitrinite in this coaly succession. Coal macerals do not occur isolated from one another but instead appear intimately associated with different macerals. These maceral associations are termed microlithotypes by Stach et al., (1982) and are also denominated organic facies of coals by Jones (1987).

The Almond coals are characterized by the predominance of three particular microlithotypes. The microlithotypes (using Diessel's terminology) are: 1) Clarite composed of desmocollinite and liptinite and

illustrated in photomicrograph 2; 2) Telite composed of telinite (or telocollinite) showed by photomicrograph in FIGURE 10; and 3) the maceral-mineral association of vitrinite and pyrite as illustrated by photomicrograph in FIGURE 11. A less abundant microlithotype is duroclarite, which is a trimaceralic microlithotype with a dominance of vitrinite.

The increasing upward trends for both desmocollinite and liptinite macerals are due to the marine-influenced environment that resulted from the overall transgression during deposition of the Almond Formation. As the sea level rises, the pH of the water in the swamps and lagoons increases to a nearly neutral condition, and the preservation of liptinite and hydrogen-rich macerals is favored.

The limit between the Lower and Middle Almond units is placed several feet above of Olson's limit. This flooding surface is clearly indicated by the appearance of desmocollinite as shown in FIGURE 12.

Vitrinite Reflectance

The vitrinite reflectance data are reported on Table 2 and plotted against depth in FIGURE 12, which

TABLE 2. Vitrinite reflectance data of the Almond Formation at UW #4 well

Depth (ft)	R _{min} (%)	R _{max} (%)	R _o (%)	Std. Dev.
97	0.40	0.55	0.46	0.06
100	0.49	0.62	0.55	0.04
125	0.47	0.58	0.52	0.04
129	0.41	0.58	0.47	0.04
259	0.46	0.6	0.53	0.04
316	0.48	0.8	0.56	0.07
323	0.52	0.75	0.59	0.04
375	0.52	0.71	0.6	0.04
392	0.42	0.64	0.52	0.06
417	0.52	0.71	0.63	0.04
424	0.49	0.7	0.59	0.04
465	0.54	0.62	0.57	0.03
467	0.38	0.68	0.58	0.07
499	0.4	0.65	0.56	0.07
501	0.5	0.8	0.58	0.06
549	0.49	0.63	0.56	0.03
580	0.52	1.29	0.6	0.13
2669	0.55	0.95	0.65	0.06
3078	0.54	0.69	0.62	0.03

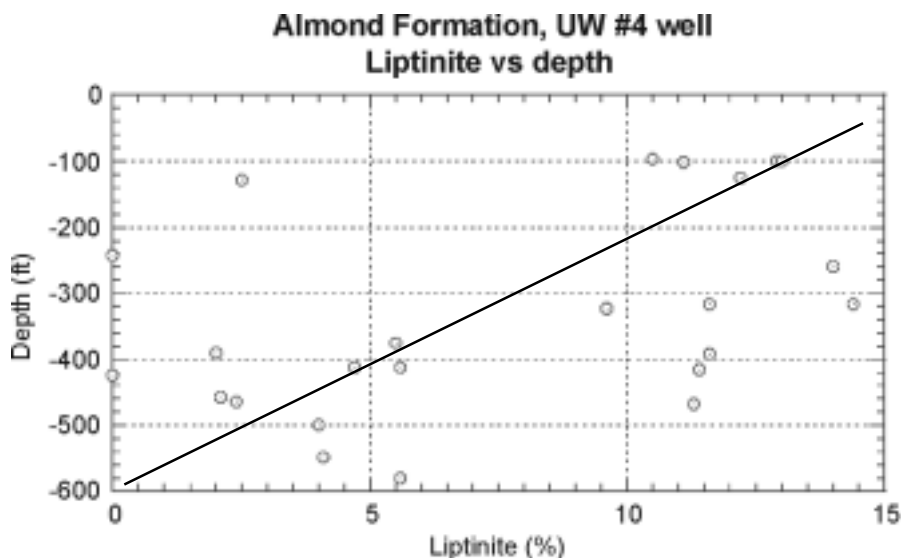


FIGURE 6. Liptinite maceral versus depth in coal beds of the UW # 4 well. Notice the upward increasing trend.

illustrates a clear upward decreasing trend of vitrinite reflectance that reflects the overall transgression of the Almond Formation. In fact, coal beds from the Lower Almond exhibit a vitrinite reflectance (R_o) value of 0.58 to 0.63%. On the other hand, coal beds from the Upper Almond exhibit R_o value between 0.47 and 0.52%. This situation clearly indicates the suppression of vitrinite reflectance due to the presence of desmocollinite. Carr (2000) discusses the vitrinite suppression due to the presence of liptinite maceral within vitrinite particles. Also, Diessel (1992) explains how coal beds with a marine roof exhibit vitrinite reflectance suppression from bottom to top, reflects a change in the geochemical environments.

GEOCHEMISTRY

The following geochemical analyses were carried out for coals and shales: (1) anhydrous pyrolysis, (2) Total Organic Carbon (TOC), and (3) The elemental analysis of Carbon, Nitrogen and Hydrogen. The anhydrous pyrolysis analyses provided the following geochemical parameters: production index [$PI = S_1 / (S_1 + S_2)$], where S_1 represents the hydrocarbon already generated and now held in the source rock, and S_2 correspond to the hydrocarbon generated during pyrolysis of the sample, genetic potential ($GP = S_1 + S_2$), and hydrogen index ($HI = S_2 / TOC$).

TABLE 3 includes anhydrous pyrolysis and TOC data, and TABLE 4 includes the elemental analysis data.

The geochemical interpretation was made by grouping the geochemical data according to the sequences of the Almond Formation.

The lower Almond contains coal beds and coaly shales with relatively low TOC values between 3.5 and 65%. Only the upper most coal bed has a high TOC value of 74%. HI values range from 165 to 247. These values are relatively high and indicate a potential for wet gas and condensate.

The Middle Almond Formation presents coal and shales with TOC values ranging from 3 to 73%; the TOC values are low for the coal beds, since only one sample has a TOC value higher than 70%. The HI values range 160 to 330 mgr of hydrocarbon, with an average value of 209 mgr of hydrocarbon, indicating both gas and condensate generation potential for this sequence. In this succession two high values of HI (> 300 mg HC) mark the base and top of the middle Almond and are explained by flooding events FIGURE 14.

The Upper Almond coals have TOC values higher than 70%, and the shales present TOC between 4 and 8%. HI values range between 105 and 234 mgr of hydrocarbon but are lower than the Middle Almond. The HI peak of Figure 14 marks the boundary between the Middle and Upper sequences; the top of this sequence is not present in the UW # 4 well.

TABLE 3. TOC and anhydrous pyrolysis analyses of the Almond Formation coals

Depth	S ₁	S ₂	T _{max}	TC	TOC	HI	PI	GP	R ₀	R _{min}	R _{max}	StDev
(ft)	mg HC/g	mg HC/g	°C	(%)	(%)	Mg HC/TOC	S _P /(S ₁ +S ₂)	S ₁ +S ₂	%	%	%	
-96	0.43	3.66	434.9	5.0	3.5	104.6	0.11	4.1				
-97	1.08	111.28	429.0	72.9	72.9	152.6	0.01	112.4	0.46	0.40	0.55	0.06
-99	0.97	108.77	429.0	73.0	73.0	149.0	0.01	109.7				
-100	1.61	141.97	427.3	71.3	71.3	199.1	0.01	143.6	0.55	0.49	0.62	0.04
-125	0.35	9.53	427.6	8.8	6.4	148.9	0.04	9.9	0.52	0.47	0.58	0.04
-130	1.09	164.00	412.6	70.2	70.2	233.6	0.01	165.1	0.47	0.41	0.58	0.04
-242	0.93	130.05	423.1	73.1	73.1	177.9	0.01	131.0				
-248	0.47	15.46	430.2	8.1	8.0	193.3	0.03	15.9				
-249	0.39	6.12	431.7	4.8	4.1	149.2	0.06	6.5				
-256	0.83	148.56	428.9	74.6	74.6	199.1	0.01	149.4				
-259	1.15	139.26	421.4	50.8	50.8	274.1	0.01	140.4	0.53	0.46	0.60	0.04
-261	0.77	32.00	425.6	9.7	9.7	329.8	0.02	32.8				
-295	0.80	3.79	430.9	3.5	2.5	151.4	0.17	4.6				
-316	0.85	133.20	428.8	65.2	65.2	204.3	0.01	134.1	0.56	0.48	0.80	0.07
-323	0.80	135.41	430.3	74.2	74.2	182.5	0.01	136.2	0.59	0.52	0.75	0.04
-375	0.93	133.33	423.2	71.4	71.4	186.7	0.01	134.3	0.60	0.52	0.71	0.04
-377	0.59	28.53	427.6	17.7	17.7	161.2	0.02	29.1	0.52	0.42	0.64	0.06
-390	1.52	128.93	429.1	72.2	72.2	178.6	0.01	130.5				
-392	1.33	144.16	426.4	68.1	68.1	211.7	0.01	145.5				
-412	0.67	102.03	424.8	50.2	50.2	203.2	0.01	102.7	0.63	0.52	0.71	0.04
-427	1.52	154.21	409.7	65.1	65.1	236.9	0.01	155.7	0.59	0.49	0.70	0.04
-458	0.25	6.93	433.8	5.4	5.4	128.3	0.04	7.2				
-464	0.36	14.26	430.9	8.6	8.3	171.8	0.02	14.6				
-466	1.27	140.87	418.7	45.0	45.0	313.0	0.01	142.1	0.58	0.38	0.68	0.07
-478	0.82	10.87	428.0	22.5	22.5	48.3	0.07	11.7				
-499	0.97	158.24	412.8	66.3	66.3	238.7	0.01	159.2				
-501	1.81	124.09	424.6	73.6	73.6	168.6	0.01	125.9	0.58	0.50	0.80	0.06
-508	0.55	5.78	427.9	4.2	3.5	165.2	0.09	6.3				
-518	0.52	11.15	433.8	5.8	5.8	192.2	0.04	11.7				
-530	0.54	11.96	432.3	7.9	7.8	153.3	0.04	12.5				
-549	0.82	139.22	427.7	64.3	64.3	216.5	0.01	140.0	0.56	0.49	0.63	0.03
-580	1.97	95.68	420.0	55.5	55.5	172.4	0.02	97.6	0.60	0.52	1.29	0.13
-609	0.86	142.39	415.9	69.4	69.4	205.2	0.01	143.2				
-614	1.57	60.45	414.4	24.5	24.5	246.7	0.03	62.0				
-671	1.14	41.63	424.4	19.9	19.9	209.2	0.03	42.8				

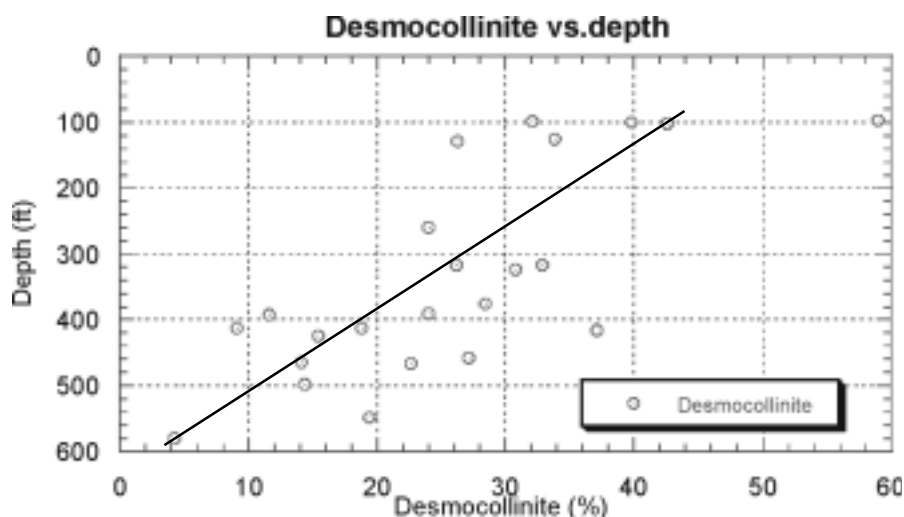


FIGURE 7. Desmocollinite maceral versus depth in the coal beds, of the UW # 4 well. Notice the upward increasing trend of desmocollinite.

The Almond formation coals (TABLE 4) present an average hydrogen content value of 5.54%, and a carbon content between 50 and 73%. The chemical composition of the Almond coals falls within the hyper-hydrous field of the Syeler's chart, (used by Diessel, 1992) see FIGURE 15. This chemical classification agrees with the organic petrography and the anhydrous pyrolysis analysis and indicates that the Almond coals were deposited under marine influence, similar to the examples discussed by Diessel (1992).

The carbon nitrogen ratio C/N has been used as an indicator of organic matter provenance. In general, an increase in the C/N ratio is related to a continental environment due to a higher content of carbon and relatively low nitrogen content. However, Tyson (1995) thinks that the C/N is not always a good indicator of organic matter provenance. The results obtained in the Almond coal do not show any particular trend.

DISCUSSION

The maceral distribution presents two distinctive trends for liptinite and desmocollinite content as illustrated in FIGURES 6 and 7. The liptinite content increases upwards in the second and third parasequences of the Almond Formation. The same trend is observed for desmocollinite. These maceral trends are indicative of depositional environments, where marine invasions changed the conditions of coal deposition from a marsh-dominated environment to a lagoon-dominated environment.

The break points of liptinite and desmocollinite trends coincide with the location of fourth-order boundaries that represent marine invasions (FIGURE 12). In conclusion the Almond coals present petrological characteristics that indicate a fresh-water or swamp environment in the first parasequence. Toward the top of the first parasequence, the environment changes from fresh-water to brackish-water, as indicated by the change in vitrinite composition from telocollinite to desmocollinite.

A fourth-order boundary marked by a marine flooding surface caused a drowning of peat deposits. The second sequence shows a succession that starts with deposition of coal beds in back-barrier environment with brackish-water composition that changes to a lagoonal environment with higher salinity of the water. The change from back-barrier to lagoon is indicated by several factors such as an upward increasing trend of liptinite and desmocollinite content and a decreasing tendency of vitrinite reflectance from bottom to top of the second sequence.

The third parasequence contains few coal beds interbedded with marine shales, implying that these coals were deposited in a marine influenced embayment environment. As in the previous sequences, the liptinite and desmocollinite content increases upward, and the vitrinite reflectance exhibits an upward decreasing trend.

TABLE 4. Nitrogen, Carbon, and Hydrogen analyses of the Almond Formation

Depth (ft)	Nitrogen (%) daf	Carbon (%) daf	Hydrogen (%) daf
96	0.00	54.85	0.00
97	0.62	75.84	5.12
99	0.98	74.52	5.32
100	1.17	73.51	5.20
125	0.00	74.27	0.00
130	1.48	74.11	5.39
242	1.67	74.75	5.12
248	1.28	56.68	8.54
249	0.57	57.12	0.00
259	1.85	72.31	5.75
261	1.42	56.35	8.05
295	0.28	45.60	0.00
317	1.35	69.06	5.13
325	1.53	78.91	5.11
375	1.34	72.67	5.04
377	1.90	71.20	6.48
390	1.55	75.55	5.50
392	1.61	76.58	5.75
416	1.60	75.66	5.56
427	1.47	71.77	5.37
458	0.00	30.25	10.22
464	0.00	58.41	8.97
467	0.91	52.12	5.35
478	1.75	143.17	9.00
499	1.43	77.67	6.03
502	1.74	77.90	5.48
508	0.00	50.46	0.00
518	0.00	47.15	10.18
530	1.18	56.68	8.56
549	1.24	75.81	5.83
557	1.86	79.16	5.54
580	1.02	75.56	5.89
609	1.17	75.78	6.04
614	1.36	69.37	6.59
671	0.75	69.02	6.96

The Hydrogen Index of the Almond coals ranges between 100 and 330 mg of hydrocarbon. FIGURE 14 shows two prominent HI peaks at 260 and 470 feet deep. The location of these two HI peaks coincides with the position of marine invasions or tidal sediments that correspond to flooding surfaces. It is also remarkable that 43% of the coal beds present HI higher than 200 mg of hydrocarbon, indicating oil-prone coals, as discussed by García-González et al; (1993) and García-González et al. (1997).

The Almond Formation is a good example of a succession in which the coal beds formed in a

transgressive systems tract. At least three sequences have been identified in the Almond Formation. The lower parasequences presents coal beds formed during the initial phase of sea level rise and corresponds to a transgressive system tract TST, where coal beds appear at the top of the sequence.

The Middle Almond Formation corresponds to the second sequence. This was deposited also during sea level rise and corresponds to a high stand system tract (HST). During HST the coal deposition resulted in thin and multiple coal beds due a lack of accommodation space and or high rate of deposition that drowned the peat deposits. The top of this parasequence is marked by the appearance of tidal sandy deposits, which mark the upper boundary of this parasequence.

The Upper Almond was also deposited during sea level rise in an HST; the coal beds are also thin and occur interstratified with silty shales of lagoon environment and marine shales at the top of the third parasequence. The coal beds are less numerous than the Middle Almond due the frequent marine incursions that drowned lagoons and back barrier swamps.

Implications For Coal Bed Methane Exploration

The petrographic and geochemical characteristics of the Almond Formation coals indicate that these coals are rich in lipid compounds, which have a high generation potential not only for methane but also for condensates.

FIGURE 16 illustrates the volume of methane generated by different macerals; this figure shows that liptinite maceral generates up to one order of magnitude more gas than the vitrinite macerals. Since the Almond coals are extremely rich in desmocolinite, these coal beds therefore possess greater gas generation potential than the coal bed from the Rock Springs, Lance and Fort Union Formations.

The anhydrous pyrolysis (Rock Eval) analyses of the Almond Formation coals also show that some coals exhibit a hydrogen index above 200 mgr of hydrocarbon (TABLE 1). In addition, the Almond coal samples from the Red Desert and Mille Creek areas present HI values ranging between 150 and 311 mgr of hydrocarbons. In contrast, the HI values of Rock Springs, Lance and Fort Union coals are generally lower than 100 mgr of hydrocarbon.

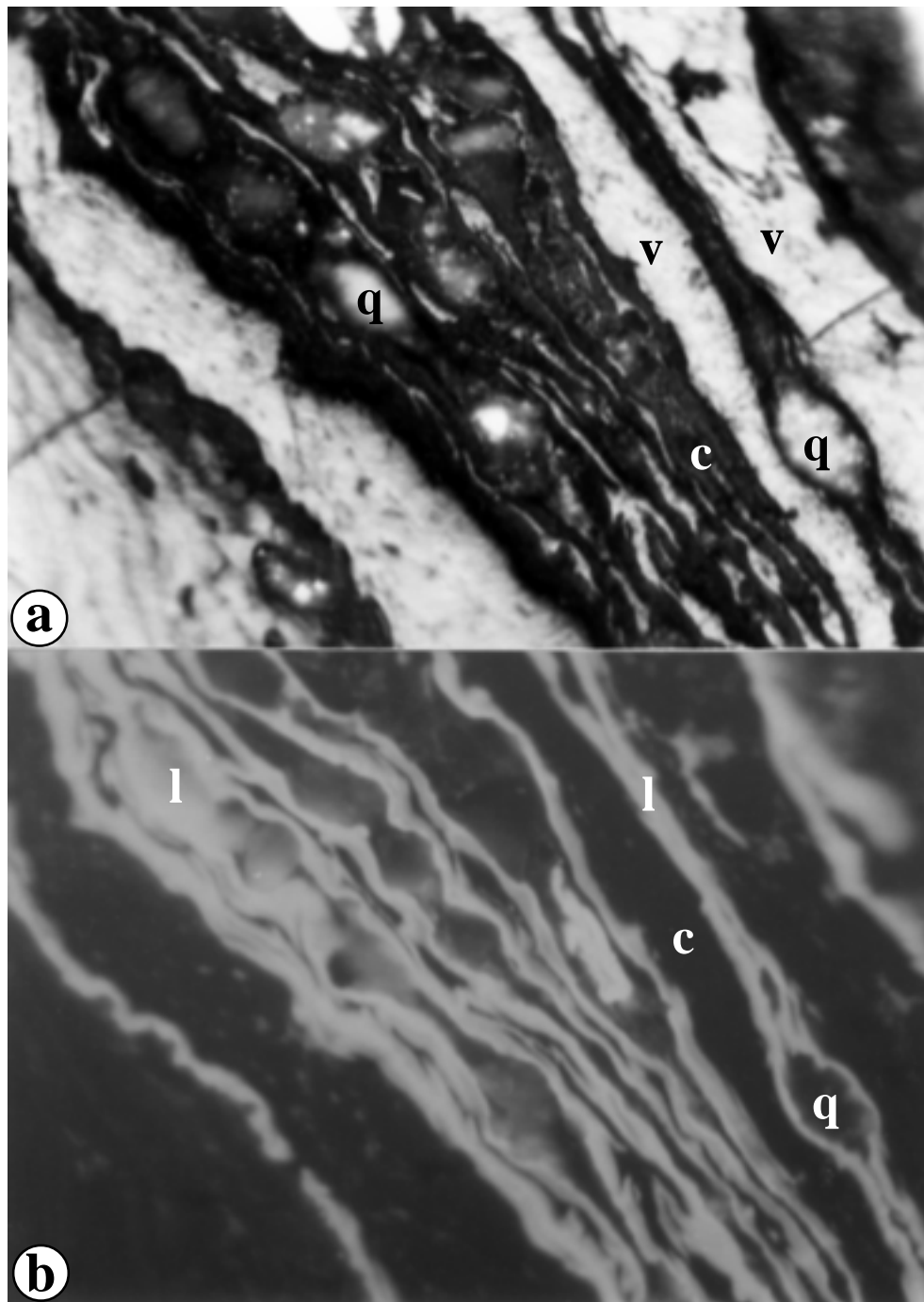


FIGURE 8. a. Coaly shale of the Almond Formation at 200 feet depth. Notice the interbedding of vitrinite, liptinite and clays. Vitrinite (v); liptinite (l); clays (c); quartz (q). b. Same field as a showing fluorescence of liptinite (l). The length of the long axis is 150 μ m

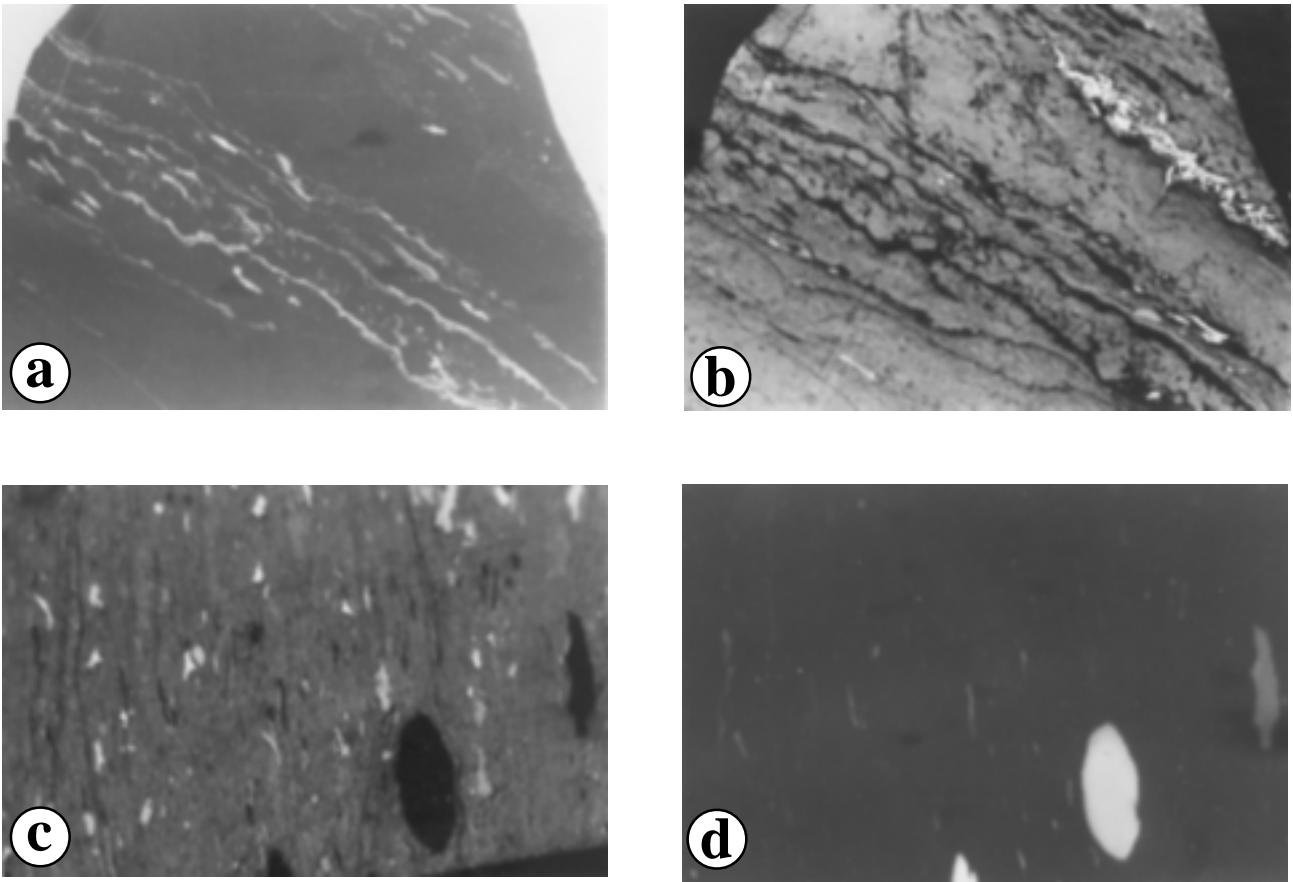


FIGURE 9. **a.** Desmocollinite under blue light showing the fluorescence of cutinite and other liptinite particles. **b.** Same field as A. under white light illustrating the characteristic texture of Desmocollinite. Pictures A and D are from a coal bed of UW # 4 well, at 323 feet deep. **c.** Desmocollinite with abundant minute particles of liptinite and a large particle of Resinite. **d.** Same field as C under blue light showing the fluorescence of Resinite and other liptinite macerals. Pictures C and D are from a coal bed at 97 feet deep of UW # 4 well. The length of the long axis is 500 μm for these four pictures.

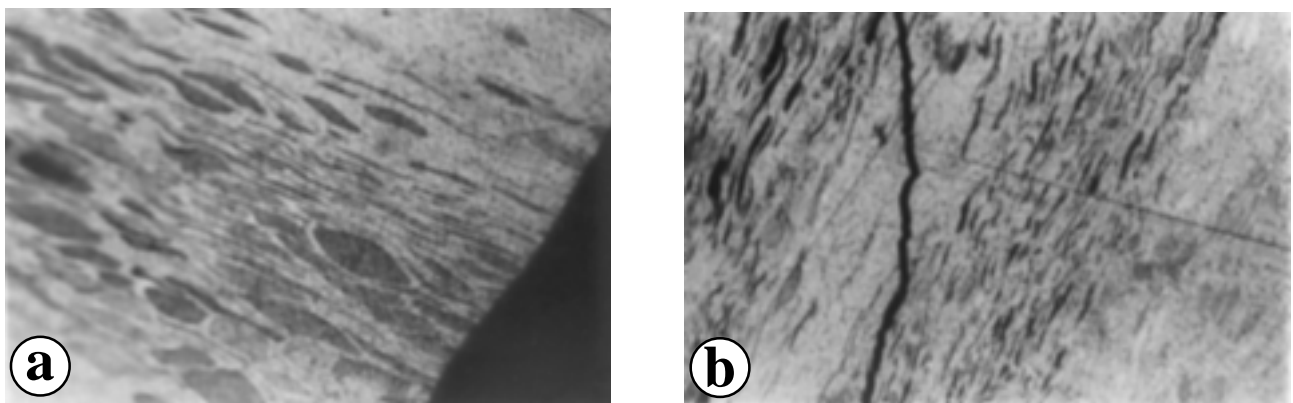


FIGURE 10. **a.** Almond coal at 125 feet deep of UW #4 well. Detail of telocollinite, showing the cell structures. **b.** Almond coal at 129 feet deep, illustrating telocollinite and liptinite macerals. The length of the long axis is 500 μm

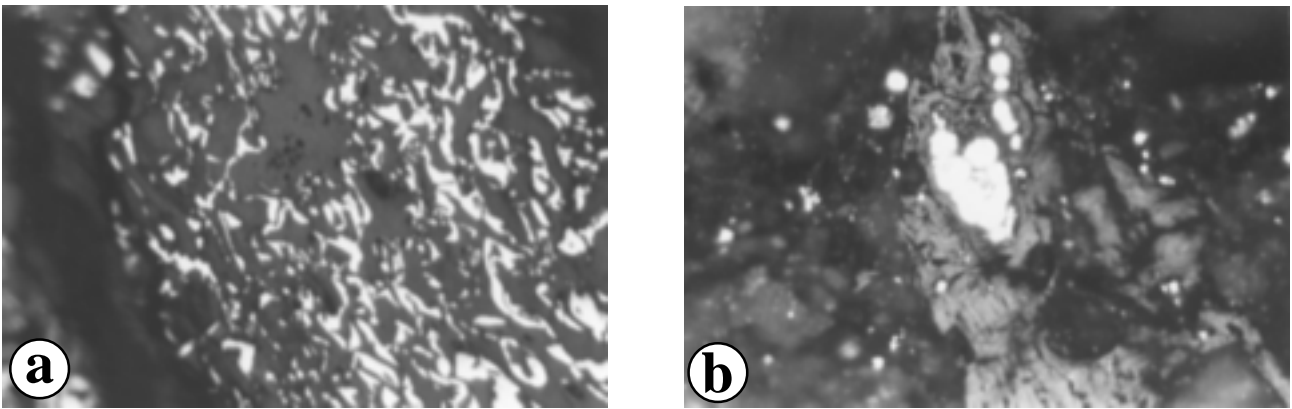


FIGURE 11. a. Almond coal at 100 feet deep. UW # 4 well. Detail of pyrite and vitrinite. b. Almond coal bed at 225 feet deep. Detail of pyrite framboids that are characteristic of anoxic environments.

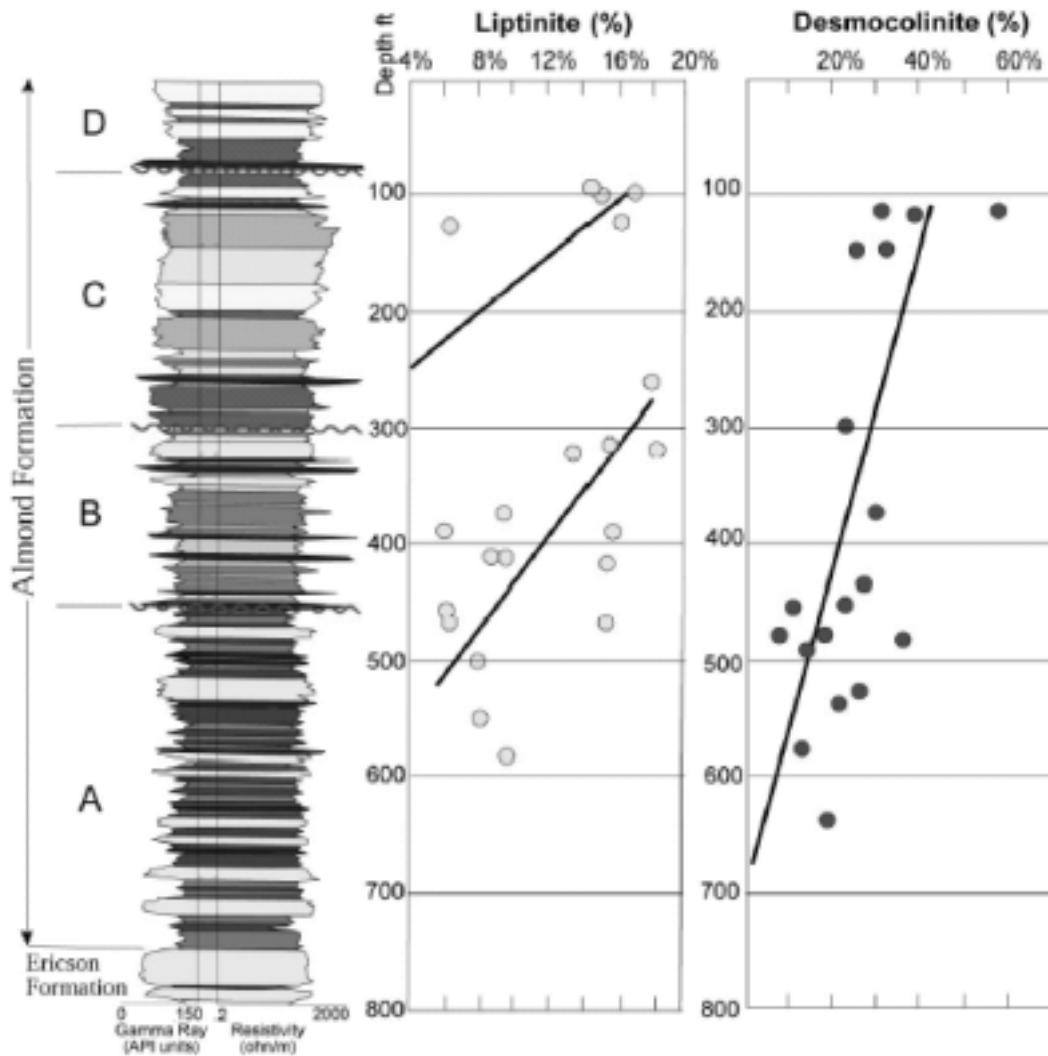


FIGURE 12. The figure illustrates how the maceral trends content is used to point the boundaries between four-order sequences in the UW # 4 well. Both macerals liptinite (in yellow dots) and desmocollinite (in blue dots) increase upward due to overall transgression. Consequently, the preservation of hydrogen-rich maceral is favored due to the water Ph, which goes from acid to near neutral as marine water invades some the back-barrier areas.

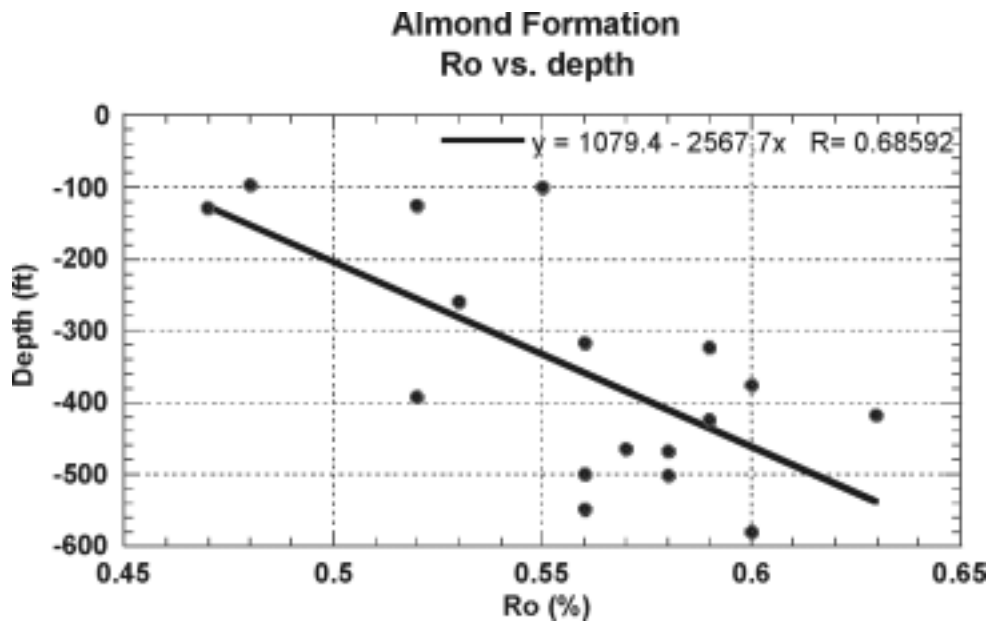


FIGURE 13. Vitrinite reflectance (Ro) versus depth, in the coal beds of the UW # 4 well. Notice the upward decreasing trend of Ro due to reflectance suppression. This vitrinite reflectance suppression is due to abundance of lipid-like maceral such as liptinite and desmocollinite.

Consequently, the generation potential of the Rock Springs, Lance and Fort Union Formations is limited compared to the Almond Formation coals. However, the thickness of the individual coal seams, make some Fort Union coal seams good prospect for CBM exploration.

CONCLUSIONS

The occurrence of organic facies (defined with geochemical and maceral analyses) is related to four-order parasequences of the Almond Formation. Similarly, the Hydrogen Index and maceral analyses are useful in identifying four-order unconformities.

The second and third parasequence of the Almond Formation show a clear upward trend of liptinite and desmocollinite, which are explained by deposition of organic matter during a transgressive stage that increase the marine influence from bottom to top of each parasequence of the Almond Formation (FIGURES 6 and 7).

The Hydrogen Index distribution shows two distinctive peaks that coincide with marine flooding surfaces marking the top of the first and second parasequences (FIGURE 14).

The vitrinite reflectance shows a decreasing trend from bottom to top of the parasequences, a trend that is also due to the accumulation and preservation of hydrogen-rich desmocollinite.

The Almond coals present an abundant content of desmocollinite (vitrodertinite), which indicates a high input of grass and algae vegetation characteristic of marsh and lagoon environments. The high liptinite and or desmocollinite content is the result of the vegetation assemblage in a marsh and swamp-marsh-lagoon complex.

The Sequence stratigraphic framework can help to predict the special distribution of source rocks, including their characteristics regarding quality and oil/gas generation potential. In the present case, it is observed that the best oil-prone shales and oil-prone coals are deposited in transgressive sequence tracts toward the top of each parasequence.

The presence of high desmocollinite content is typical of transgressive coals with marine roof, as is the case of the Almond coals from the second and third parasequences. Diessel (1992) reports similar findings in an example from marine-influenced coals from Australia.

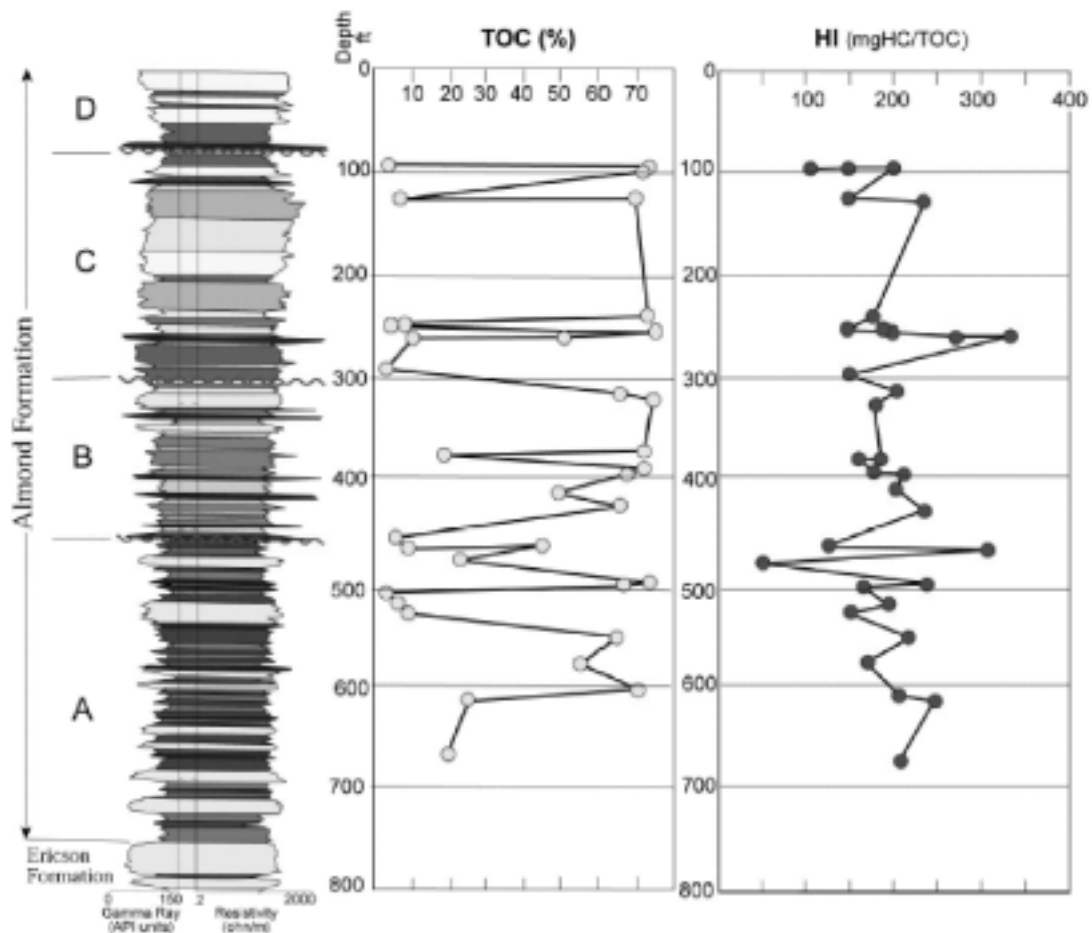


FIGURE 14. Almond Formation Facies, TOC analysis and hydrogen index of the UW # 4 well. Notice how the hydrogen index data can be used to point the boundaries between the first and second and the second and third parasequences in the Almond Formation

Select'chart, Hydrogen versus Carbon in coals

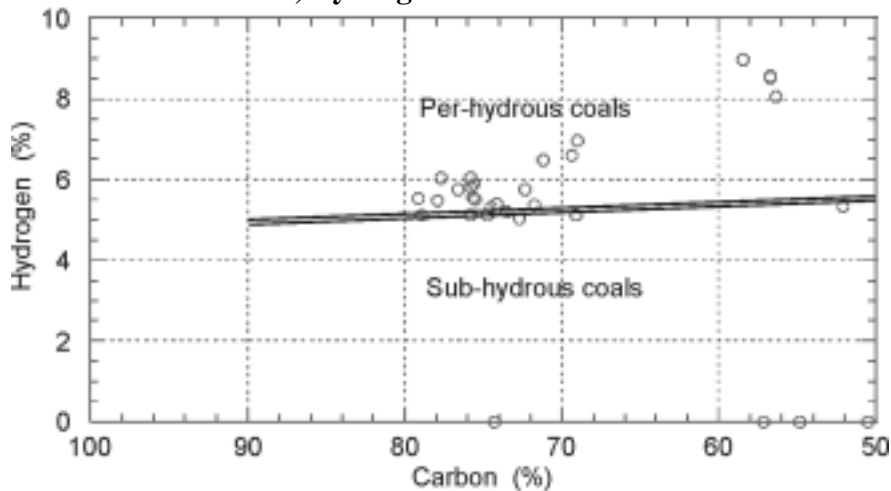


FIGURE 15. Saylor's Chart illustrating the per-hydrous characteristic of the Almond Formation coals.

HI results of the Almond Formation in the UW # 4 well show two distinctive peaks that determine the position of two main flooding surfaces due to marine invasions (FIGURE 14). In the same way, the break point of the liptinite and desmocollinite trends coincides with the parasequence boundaries, which are four-order unconformities.

According to Olson and Martisen (1999), there could be more than three four-order unconformities in the Almond Formation; however, these unconformities are impossible to identify with HI or organic petrography. This situation is explained by the location of the UW # 4 well that cored a section very close to the shoreline where some of the four-order unconformities merge.

In sum, the Almond coals were deposited in a transgressive sequence stage, which controlled the preservation of liptinite and desmocollinite macerals. This maceral composition is also shown by the Hydrogen Index trend. These characteristics make the Almond Formation coals an excellent prospect for coal bed methane and condensates.

ACKNOWLEDGEMENTS

I wish to thank Dr Dag Nummedal IER director, and Professor Ronald Steel of the University of Wyoming for their useful discussions that improved this paper. Also I wish to thank the Institute of Energy Research (IER) and Anadarko Petroleum Corporation for the generous funding of this research project. Also I wish to thank Dr. Steven Boese of the University of Wyoming for his analytical help.

REFERENCES

- Carr, D.A. (2000). Suppression and retardation of vitrinite reflectance, Part I. Formation and significance for Hydrocarbon Generation, in: *Journal of Petroleum Geology*, vol. 23 (3), pp. 313-343.
- Diessel, C.F.K. (1992). *Coal-Bearing Depositional Systems*, Springer-Verlag, Berlin, 721 p.
- Flores, R.M. (1978). Barrier and back-barrier environments of the deposition of the Upper Cretaceous Almond Formation, Rock Springs Uplift, Wyoming: *The Rocky Mountain Geologists*, v. 15, pp. 57-65.

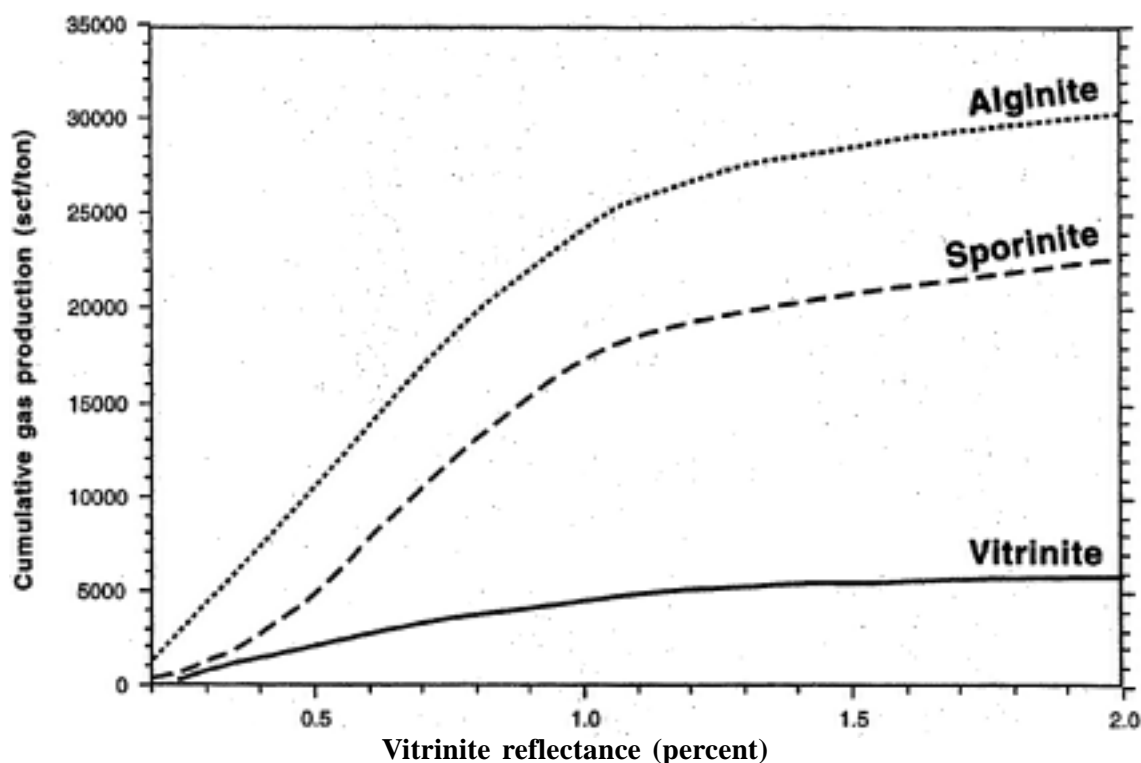


FIGURE 16. Cumulative gas production versus vitrinite reflectance. This diagram illustrates the large volume of gases generated by liptinite macerals (alginite and sporinite). (From data of Levine, 1992)

- García-González, M., McGowan, D. Surdam, R. C. (1993). Coal as a source rock of petroleum and gas; a comparison between natural and artificial maturation of the Almond Formation coals, Greater Green River Basin in Wyoming: in Howell, D., et al., editor *The Future of the Energy Gases*, U.S. Geological Survey professional paper v. 1570, pp. 405-437.
- García-González, M., Surdam, R. C., and Lee, M. L. (1997). Generation and Expulsion of petroleum and gas from Almond Formation coal, Greater Green River Basin, Wyoming, in: *AAPG bulletin* v. 81, pp. 62-81.
- Gill, J. R., E. A. Merewether, and W. A. Cobban. (1970). Stratigraphy and Nomenclature of some Upper Cretaceous and lower Tertiary rocks in south-central Wyoming: *USGS professional paper* 667, 53 p.
- Jones, R.W. (1987). Organic facies, in *Advances in Petroleum Geochemistry 2* (eds J. Brooks, and D. Welte), Academic Press, London, pp. 1-90.
- Levine, J. R. (1992) Petrologic controls on reservoir characteristics of coal beds, in Ayers, W. B., Jr., Kaiser, W. R., and Levine, J.R., eds. *Coalbed methane: depositional, hydrologic and petrologic controls on reservoirs characteristics of coalbeds: AAPG 1992 Annual convention, Short Course N0 13*, pp. 58-160.
- Meyer, W. C. (1977). Environmental analysis of the Almond Formation (Upper Cretaceous) from the Rock Springs Uplift, Wyoming: Tulsa University, Ph.D. Dissertation, and 336 p.
- Obradovich, J. D. (1993). A Cretaceous time scale, in: *WGE Cadwell and E.G. Kauffman, eds., The Evolution of the Western Interior Basin: Geological Association of Canada Special Publication 39*, pp. 379-396.
- Olson, M. (1999). Facies Architecture of the Almond Formation, Southwest Wyoming, M.Sc. thesis, University of Wyoming, 111 p.
- Olson, M., Martinsen, R. (1999). Facies Architecture and sequence stratigraphy of the Almond formation, Southwestern Wyoming. In: *American Association of petroleum geologists, 1999, Annual meeting Expanded abstract* p. A102-13.
- Roehler, H. W. (1990). Stratigraphy of the Mesaverde Group in the central and eastern Greater Green River Basin, Wyoming, Colorado, Utah: U.S.G.S. professional paper 1508, 52p.
- Stach, E., Mackowssky, M.T., Teichmuller, M., Taylor, G.H., et al. (1982). *Stach's Textbook of Coal Petrology*, 3rd ed., Borntraeger, Berlin.
- Tyler, R., Ambrose, W. A., Scott, A. R. and Kaiser, W. R. (1992). Evaluation of Coalbed Methane Potential in the Greater Green River, Piance, Powder River, and Raton Basins. In: *Wyoming Geological Association Guidebook, Rediscover the Rockies*, pp. 269-302.
- Tyson, R.V. (1995). *Sedimentary Organic Matter*, Chapman & Hall, London, 615 p.
- Van Horne, M. D. (1979). Stratigraphic relationships and depositional environments of the Almond and associated formations, east-central flank of the Rock Springs Uplift, unpublished M.Sc. thesis, Colorado School of Mines, 124 p.
- Weimer, R. J., (1965). Stratigraphy and petroleum occurrences, Almond and Lewis Formations (Upper Cretaceous), Waster Arch, Wyoming: *Wyoming Geological Association 19th Annual Field Conference Guidebook*, pp. 65-81.
- Weimer, R. J. (1988). Record of relative sea-level changes, Cretaceous of Western Interior, USA: *Sea-level Changes - an integrated approach, SEPM Special Publication No. 42*, pp. 285-288.

Trabajo recibido: Agosto 27 de 2003
Trabajo aceptado: Octubre 5 de 2004